

# Exploring Disentangled and Controllable Human Image Synthesis: From End-to-End to Stage-by-Stage

ZHENGWENTAI SUN, SSE, CUHKSZ, China and FNii, CUHKSZ, China  
 CHENGHONG LI, SSE, CUHKSZ, China and FNii, CUHKSZ, China  
 HONGJIE LIAO, SSE, CUHKSZ, China and FNii, CUHKSZ, China  
 XIHE YANG, SSE, CUHKSZ, China and FNii, CUHKSZ, China  
 KERU ZHENG, SME, CUHKSZ, China  
 HEYUAN LI, SSE, CUHKSZ, China and FNii, CUHKSZ, China  
 YIHAO ZHI, SSE, CUHKSZ, China and FNii, CUHKSZ, China  
 SHULIANG NING, SSE, CUHKSZ, China and FNii, CUHKSZ, China  
 SHUGUANG CUI, SSE, CUHKSZ, China and FNii, CUHKSZ, China  
 XIAOGUANG HAN\*, SSE, CUHKSZ, China and FNii, CUHKSZ, China

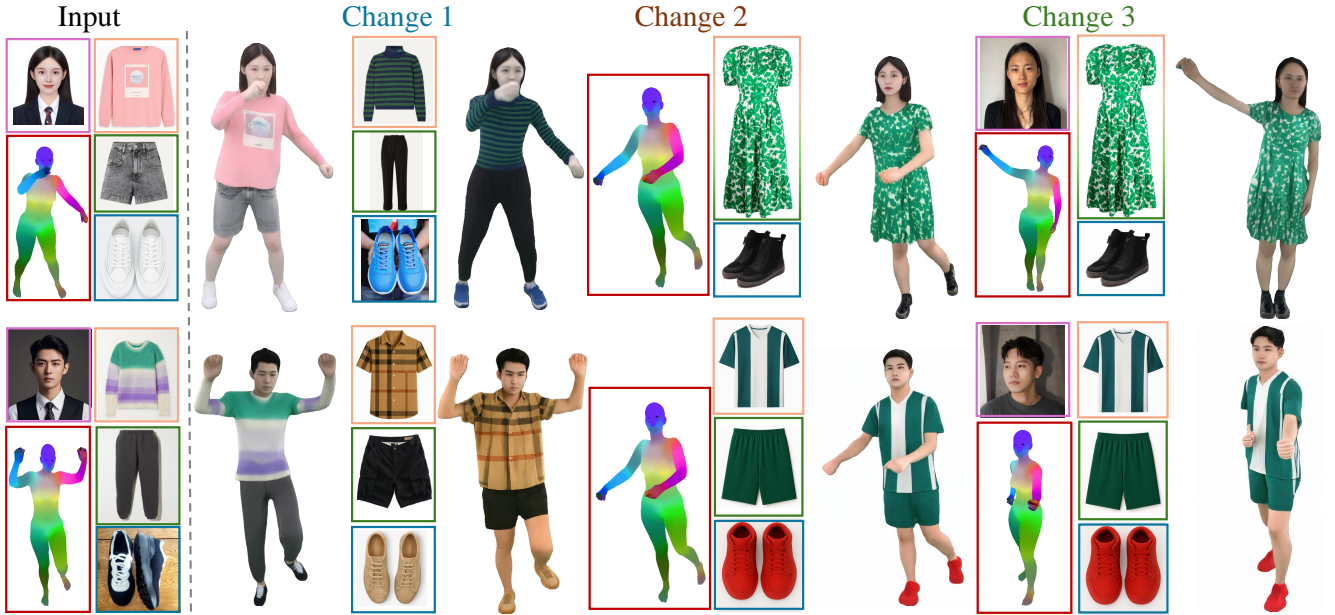


Fig. 1. We propose a new task focused on explicit disentanglement of key human attributes within a unified framework, enabling fine-grained controllability in human synthesis. Moreover, we explore to train an end-to-end model and further design a stage-by-stage pipeline for generating human images with customizable inputs, offering enhanced flexibility and superior control over the synthesis process.

Achieving fine-grained controllability in human image synthesis is a long-standing challenge in computer vision. Existing methods primarily focus on either facial synthesis or near-frontal body generation, with limited ability to simultaneously control key factors such as viewpoint, pose, clothing, and identity in a disentangled manner. In this paper, we introduce a new disentangled and controllable human synthesis task, which explicitly separates and manipulates these four factors within a unified framework. We first develop an end-to-end generative model trained on MVHumanNet for factor disentanglement. However, the domain gap between MVHumanNet and in-the-wild data produces unsatisfactory results, motivating the exploration of virtual try-on (VTON) dataset as a potential solution. Through experiments, we observe that simply incorporating the VTON dataset as additional

data to train the end-to-end model degrades performance, primarily due to the inconsistency in data forms between the two datasets, which disrupts the disentanglement process. To better leverage both datasets, we propose a stage-by-stage framework that decomposes human image generation into three sequential steps: clothed A-pose generation, back-view synthesis, and pose and view control. This structured pipeline enables better dataset utilization at different stages, significantly improving controllability and generalization, especially for in-the-wild scenarios. Extensive experiments demonstrate that our stage-by-stage approach outperforms end-to-end models in both visual fidelity and disentanglement quality, offering a scalable solution for real-world tasks. Additional demos are available on the project page: <https://taited.github.io/discohuman-project/>.

\*Corresponding author: Xiaoguang Han (hanxiaoguang@cuhk.edu.cn).

Additional Key Words and Phrases: human synthesis, generative models.

## 1 INTRODUCTION

Synthesizing human-centric images is crucial for various applications like virtual reality, the metaverse, video games, and digital fashion. Advances in GANs [Goodfellow et al. 2014; Karras et al. 2020] and large-scale facial datasets [Karras et al. 2019; Liu et al. 2015] have enabled realistic face generation [Karras et al. 2018], with subsequent research focusing on controlling facial appearances and expressions [Choi et al. 2018; Lu et al. 2018; Yang et al. 2020], though often limited to frontal views. The introduction of 3D-aware GANs, EG3D [Chan et al. 2022], brought view controllability, paving the way for unified control over viewpoint, expression, and appearance [An et al. 2023; Bai and Shen 2024; Li et al. 2024; Lin et al. 2022; Xie et al. 2023]. Compared with human faces, full-body image generation is more complex due to clothing variations and pose deformations.

Early GAN-based full-body image generation methods [Frühstück et al. 2022; Fu et al. 2022; Sarkar et al. 2021] supporting pose or appearance editing but restricted to near-frontal views. Following the key idea of EG3D [Chan et al. 2022], EVA3D [Hong et al. 2023] also tried to further enable view controllability of human image generation. There are also a specific topic in this area which focus on clothing image synthesis, i.e., virtual try-on [Choi et al. 2021, 2025; Lee et al. 2022; Morelli et al. 2022]. To achieve free-view human image synthesis, disentanglement and controllability have been key research focuses. However, a unified framework addressing all requirements remains challenging, primarily due to the lack of datasets with disentangled factors. The recent release of the multi-view human video dataset, MVHumanNet [Li et al. 2025; Xiong et al. 2024], provides the possibility to take a step forward in this research direction.

To achieve fine-grained controllability over human synthesis, we propose a task that emphasizes explicit disentanglement of facial identity, clothing, pose, and viewpoint within a unified framework. A natural approach to solving this problem is to train an end-to-end model that synthesizes human images while explicitly conditioning on these factors. We attempted to conduct experiments on MVHumanNet to train an end-to-end model. While the model demonstrates a degree of controllability, its robustness and generalizability remain limited when trained exclusively on this dataset. These limitations primarily stem from inherent issues within the dataset itself. Specifically, MVHumanNet is collected in an indoor environment, which introduces a domain gap when compared to in-the-wild data.

Given these challenges, we explore to incorporate VTON dataset, which contains high-quality clothing images with more detailed textures, combined with MVHumanNet to train end-to-end model. However, our experiments reveal that simply incorporating VTON dataset as additional data to train end-to-end model result in performance degradation rather than improvement. We attribute this decline to the inconsistency in data forms between the two datasets when training the end-to-end model with multiple conditioning factors. Instead of relying on a single end-to-end model, we explore to decompose the synthesis process into sequential stages, with each step focusing on a specific sub-task. This approach offers two

advantages: **1)** it enables better dataset utilization by allowing different datasets to specialize in sub-tasks, **2)** improves factor separation by explicitly handling each attribute at distinct stages.

Building on this framework, we designed a three-stage pipeline for generating human images with arbitrary facial identity, clothing, pose and view as input (See Fig. 1). The first stage generates a clothed A-pose human with a specified face and shoes, trained on the VTON dataset. Next, the second stage synthesizes the back view of the human using the MVHumanNet dataset. Finally, the third stage enables the generation of a human image in an arbitrary pose and viewpoint by combining the VTON and MVHumanNet datasets. To condition human synthesis on pose and viewpoint control, we use the 3D parametric model SMPLX [Pavlakos et al. 2019], and render the SMPLX mesh from a given viewpoint and apply a UV-based texture encoding, where each body part is assigned a unique color-coded coordinate. With these structured controls, we implement a diffusion transformer (DiT)-based [Peebles and Xie 2023] architecture for back-view and free-view human synthesis, which integrates these disentangled factors into the synthesis pipeline. By incorporating these structured controls, our approach enables fine-grained manipulation of multiple human attributes within a unified framework. Our experiments demonstrate that, even when using a network structure similar to the end-to-end model, the stage-by-stage approach exhibits significantly better generalizability. This suggests that a stage-by-stage framework can more effectively utilize available data by assigning different datasets to specialized sub-tasks. We also observe that as the conditioning in the third stage becomes simpler, training by combining the MVHumanNet and VTON datasets leads to improved performance compared to training solely on the MVHumanNet dataset.

The contribution can be summarized as follows:

- We introduce a new and challenging task in human image synthesis that aims to achieve explicit disentanglement and control over viewpoint, pose, clothing, and identity within a unified framework.
- We explore a novel end-to-end model that can address the disentangled and controllable human synthesis task and further propose a stage-by-stage framework that enhances control over pose and viewpoint, significantly improving generalizability, particularly for in-the-wild scenarios.
- Our experiments demonstrate that our methods achieve effective disentanglement, outperforming existing methods in view and pose control. We hope that our experiments and discussion on end-to-end versus stage-by-stage methods will inspire relevant human synthesis research.

## 2 RELATED WORK

### 2.1 Human Synthesis

In the realm of human synthesis, recent works [Dong et al. 2023; Frühstück et al. 2022; Fu et al. 2022; Hong et al. 2023; Sarkar et al. 2021; Xiong et al. 2023; Zhang et al. 2023a,d] have advanced the field by focusing on generating high-quality, full-body human images with diverse identities, hairstyles, garments, and poses. StyleGan-Human [Fu et al. 2022] adopts a data-centric perspective to examine the data factors influencing image generation based on the

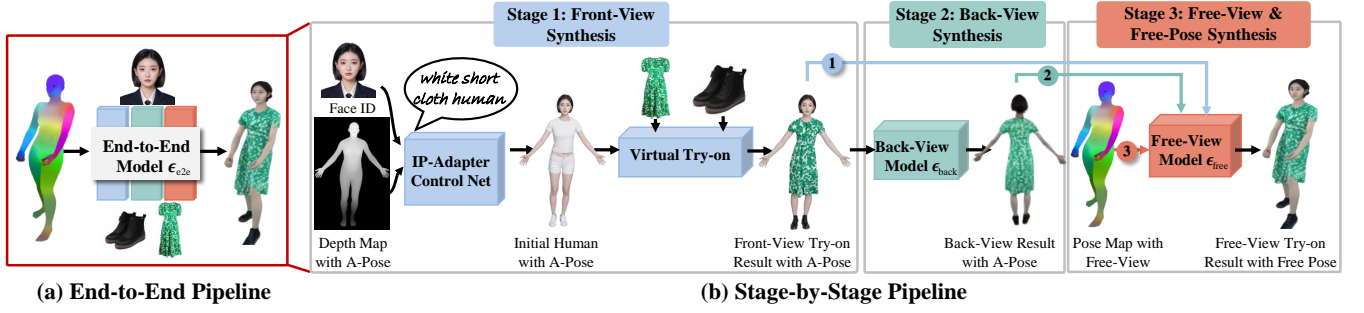


Fig. 2. Overview of the proposed pipelines. (a) The end-to-end pipeline directly synthesizes the final image from disentangled inputs, including a face image, clothing images, and a pose map. (b) The stage-by-stage pipeline decomposes the process into three steps: front-view synthesis with identity and clothing control, back-view synthesis, and free-view synthesis under the target pose and viewpoint. Both pipelines are implemented using DiscoHuman, with details provided in Fig. 3.

StyleGAN framework. InsetGAN [Frühstück et al. 2022] integrates multiple pre-trained GANs, with each focusing on distinct components. To achieve control over pose, local body part appearance and garment style, HumanGAN [Sarkar et al. 2021] is capable of performing all tasks related to global appearance sampling, pose transfer, part and garment transfer, as well as part sampling. EVA3D [Hong et al. 2023] and Get3DHuman [Xiong et al. 2023] expand the synthesis capabilities beyond 2D, pushing toward 3D human generation with realistic texture and pose control. EVA3D [Hong et al. 2023] incorporates a compositional human NeRF (Neural Radiance Field) representation, which divides the human body into 16 distinct parts and assigns each part an individual network. Each network models the corresponding local volume, allowing EVA3D to capture detailed textures and pose variations with high accuracy. Get3DHuman [Xiong et al. 2023], lifting StyleGAN-Human into 3D, advances full-body human synthesis and enables detailed control over body shape, garment, and even facial expression, making it highly applicable in applications like gaming and digital fashion.

## 2.2 Pose Transfer

With the rise of diffusion models, increasing research [Bhunia et al. [n. d.]; Hu 2024; Lu et al. 2024; Shen et al. 2023; Xu et al. 2024b] has focused on realistic person image generation. PIDM [Bhunia et al. [n. d.]] first explores denoising diffusion for person synthesis, demonstrating high-quality results via iterative refinement. PCDM [Shen et al. 2023] adopts a step-by-step conditional framework to enhance pose control. MagicAnimate [Xu et al. 2024b] and AnimateAnyone [Hu 2024] extend diffusion to person animation, achieving smooth pose transitions and dynamic visual effects. Champ [Zhu et al. 2024] incorporates a 3D human model into latent diffusion for enhanced 3D conditioning. Human4DiT [Shao et al. 2024] leverages diffusion transformers to synthesize 360° coherent human videos from a single image, enabling fine-grained pose and view control.

## 2.3 Virtual Try-on

Image-based virtual try-on (VTON) synthesizes realistic images by transferring garment appearances onto their bodies. Recent methods use GANs or diffusion models to improve realism and precision. GAN-based approaches like VITON-HD [Choi et al. 2021] address

high-resolution image misalignment with ALIAS normalization, while HR-VITON [Lee et al. 2022] integrates warping and segmentation into a unified try-on condition generator to reduce artifacts. However, GAN-based models often produce unnatural deformations in wild scenarios, reducing the fidelity and realism of the output result. In contrast, diffusion models have recently demonstrated strong performance in image generation. OOTDiffusion [Xu et al. 2024a] aligns garment features with bodies using Outfitting Fusion, improving realism and controllability without redundant warping. IDM-VTON [Choi et al. 2025] employs a visual encoder and parallel UNet for better garment encoding, while DressCode [Morelli et al. 2022] introduces a multi-category dataset and a Pixel-level Semantic-Aware Discriminator (PSAD) to enhance image quality.

## 3 METHOD

### 3.1 Overview

Fig. 2 provides an overview of the proposed pipelines for human image synthesis: an end-to-end pipeline and a stage-by-stage pipeline. Both pipelines leverage the proposed DiT-based model, **DiscoHuman**, which enables **disentangled** and **controllable human** image synthesis.

The end-to-end pipeline directly generates a complete human image from a set of disentangled inputs, including a face image, clothing images (upper/lower clothing or a dress, and shoes), and a pose map, allowing simultaneous control over face identity, clothing, pose, and viewpoint. In contrast, the stage-by-stage pipeline refines the synthesis process in three stages. It first generates an A-pose human image with identity and clothing control, then estimates the back view, and finally synthesizes a free-view image under a target pose and viewpoint. This decomposition enhances controllability and generalizability. DiscoHuman is adapted for the second and third stage by modifying its input configurations. Architectural details of DiscoHuman are further described in Sec. 3.2.

### 3.2 DiscoHuman

We developed DiscoHuman for disentangled and controllable human synthesis. Fig. 3 illustrates its structure. Given a set of disentangled conditions, it enables fine-grained control over appearance,

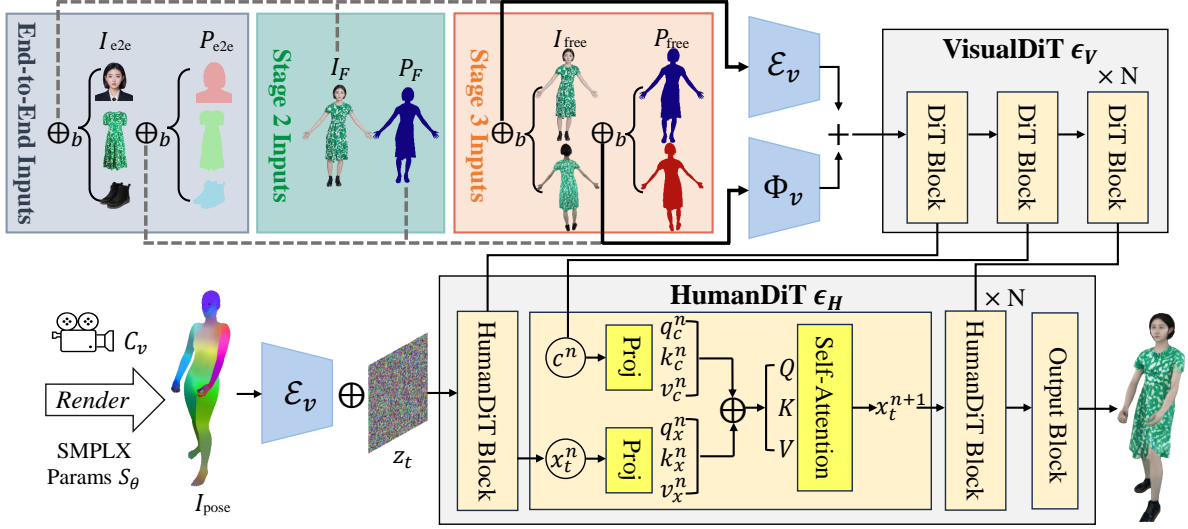


Fig. 3. DiscoHuman model  $\epsilon$  consists of a VisualDiT  $\epsilon_V$  and a HumanDiT  $\epsilon_H$ . The VisualDiT is responsible for encoding visual conditions, with different input settings depending on the pipeline or stage in which DiscoHuman is applied. The upper left blocks illustrate three possible input configurations. In this figure, the active configuration corresponds to Stage 3, while the inactive settings are indicated by grey dashed lines. To maintain simplicity, the denoising timestep  $t$  is not shown in this figure.

pose, and viewpoint in human image generation. The model consists of two key components: VisualDiT, which encodes appearance-related conditions, and HumanDiT, which synthesizes the final human image while ensuring spatial alignment with the input pose.

**VisualDiT Encoder.** The VisualDiT Encoder is a DiT-based module specifically designed for encoding visual conditions. Unlike standard DiT models, which take a noised latent as input, VisualDiT processes un-noised latents extracted from input images and conditions the denoising timestep at a fixed value  $t_0$ .

A key challenge in implementing VisualDiT lies in the variability of both the number and semantics of input conditions. For example, a sample may contain two garment images (e.g., top and bottom) or a single image (e.g., a dress). Designing separate encoders for each semantic category is computationally inefficient. To overcome this, the VisualDiT encoder employs a unified strategy. Given a set of input images  $I = \{I_1, I_2, \dots, I_n\}$ , each is encoded via a VAE encoder  $\mathcal{E}_v(\cdot)$  to produce latent representations. The corresponding segmentation masks  $P = \{P_1, P_2, \dots, P_n\}$  are one-hot encoded to indicate semantic categories. A convolutional embedding function  $\Phi_v(\cdot)$  processes these masks to align them with the image latents.

The VisualDiT Encoder then processes the concatenated image latents and embedded semantic maps, producing multi-level condition features  $c^n$  at each DiT block:

$$c^n = \epsilon_V (\mathcal{E}_v (\oplus_b I) + \Phi_v (\oplus_b P), t_0), \quad (1)$$

where the superscript  $n$  indicates the index of the DiT block,  $\epsilon_V$  denotes VisualDiT,  $\mathcal{E}_v(\cdot)$  is the VAE encoder, and  $\oplus_b$  represents batch-wise concatenation.

**HumanDiT.** The HumanDiT model synthesizes the final human image based on the multi-level condition features  $c^n$  and a viewpoint-conditioned pose representation. To achieve precise pose and viewpoint control, we utilize the 3D parametric model SMPLX [Pavlakos et al. 2019]. The SMPLX mesh is rendered under the target viewpoint, providing a structured pose representation that encodes both articulation and spatial alignment. The resulting pose map  $I_{\text{pose}}$  is then processed through the VAE encoder  $\mathcal{E}_v(\cdot)$  to ensure consistency with the visual condition features.

The HumanDiT model conditions the synthesis process on these features, formulated as:

$$\hat{\epsilon}_t = \epsilon_H (z_t \oplus \mathcal{E}_v(I_{\text{pose}}), t, c^n), \quad (2)$$

where  $\epsilon_H$  represents the HumanDiT model,  $z_t$  is a random noise latent, and  $\oplus$  denotes channel-wise concatenation. The pose map  $I_{\text{pose}}$  is processed using the VAE encoder  $\mathcal{E}_v(\cdot)$ , aligning its representation with the image features.

Within each DiT block of  $\epsilon_H$ , effective feature fusion is essential. To achieve this, the diffusion feature  $x_t^n$  and the multi-level condition features  $c^n$  are separately projected into query ( $q$ ), key ( $k$ ), and value ( $v$ ) representations, which are concatenated in a length-wise manner:

$$\mathbf{Q} = q_x^n \oplus q_c^n, \quad \mathbf{K} = k_x^n \oplus k_c^n, \quad \mathbf{V} = v_x^n \oplus v_c^n. \quad (3)$$

A self-attention mechanism is then applied to fuse these features, allowing the HumanDiT model to effectively reference the conditioning information:

$$\hat{x}_t^{n+1} = \text{softmax} \left( \frac{\mathbf{Q}\mathbf{K}^T}{\sqrt{d}} \right) \mathbf{V}. \quad (4)$$

Since concatenating  $c^n$  increases the sequence length, the excess portion is discarded after attention to maintain computational efficiency.

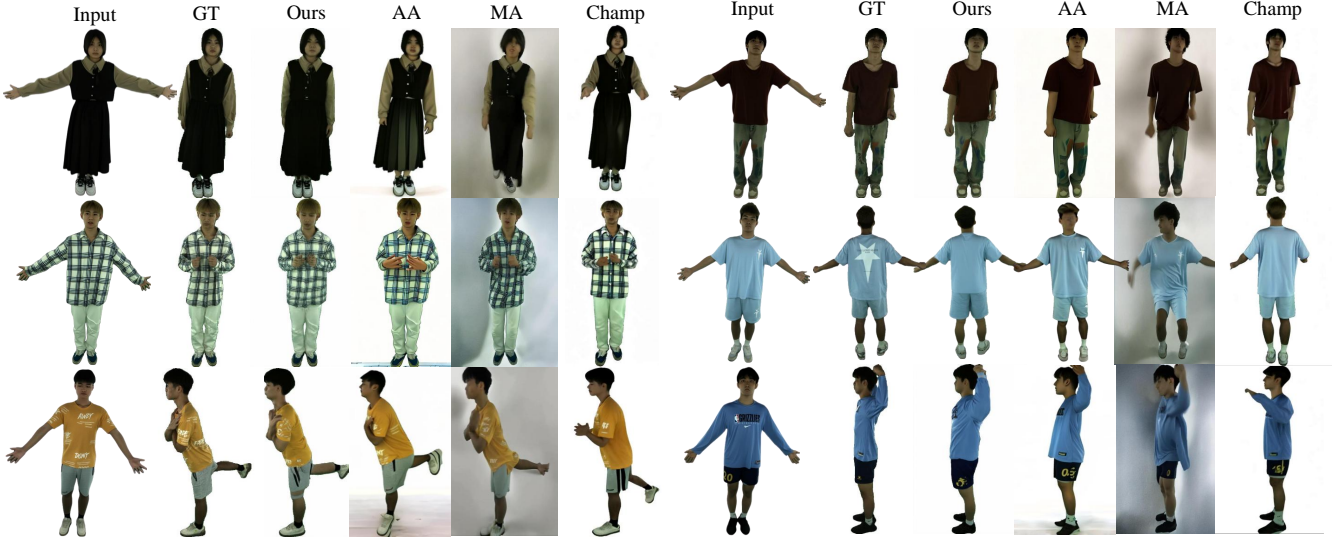


Fig. 4. Qualitative comparison of different methods on MVHumanNet [Xiong et al. 2024] datasets. Note that AA stands for AnimateAnyone and MA stands for MagicAnimate.

*Rectified Flow Loss.* To optimize the entire DiscoHuman model  $\epsilon$ , we applied rectified flow [Esser et al. 2024; Liu et al. 2022]. The forward and corresponding loss function are defined as follows:

$$\hat{\epsilon}_t = \epsilon(z_t, I_{\text{pose}}, t, I, P), \quad (5a)$$

$$\mathcal{L} = \mathbb{E}_{t, x_0, x_t} [w(t) \|\hat{\epsilon}_t - (x_t - x_0)\|^2], \quad (5b)$$

where  $w(t)$  is a weighting function [Esser et al. 2024],  $x_0$  is the latent representation of the ground truth image, and  $x_t$  represents noised  $x_0$  at timestep  $t$ .

### 3.3 End-to-End (E2E) Pipeline

In the end-to-end pipeline, we extract controllable factors from an A-pose image using SMPLX parameters and segmented face and clothing images. The inputs image and corresponding parsing maps to the VisualDiT Encoder are defined as:

$$I_{e2e} = \{I_{\text{face}}, I_{\text{upper cloth}}, I_{\text{lower cloth}}, I_{\text{dress}}, I_{\text{shoes}}\}, \quad (6a)$$

$$P_{e2e} = \{P_{\text{face}}, P_{\text{upper cloth}}, P_{\text{lower cloth}}, P_{\text{dress}}, P_{\text{shoes}}\}. \quad (6b)$$

The input settings for HumanDiT remain consistent with those described in Sec. 3.2. Since a person’s outfit consists of either separate garments (upper and lower) or a whole-body dress, we ensure consistency by inputting a black image with a semantic map labeled as pure ‘background’ whenever a clothing category is missing. To train the e2e model, the forward process is defined as follows:

$$\hat{\epsilon}_t = \epsilon_{e2e}(z_t \oplus \mathcal{E}_v(I_{\text{pose}}), t, I_{e2e}, P_{e2e}), \quad (7)$$

where  $\epsilon_{e2e}$  is the DiscoHuman model applied in end-to-end pipeline.

### 3.4 Stage-by-Stage (SBS) Pipeline

*Stage 1: Front-View Synthesis.* The first stage provides initial control over face identity and clothing. This process consists of two steps. First, IP-Adapter [Ye et al. 2023] is used to control face identity, while ControlNet [Zhang et al. 2023b] ensures that the human pose

is fixed in an A-pose. A simple text prompt is used to generate a person wearing a tight white T-shirt and trousers, which simplifies the subsequent try-on process. Next, given the target clothing, IDM-VTON [Choi et al. 2025] is applied to generate the try-on results. Since no dedicated model exists for shoe try-on, IP-Adapter with image-guided inpainting is used to apply shoes to the synthesized person.

*Stage 2: Back-View Synthesis.* The second stage synthesizes a realistic back-view image  $I_B$  of the previous generated front-view image  $I_F$ . This is achieved by reusing the DiscoHuman model with modified inputs in the VisualDiT Encoder, where the front-view image serves as the visual condition. Since only the front image is available, the corresponding semantic map is derived from its foreground segmentation as  $P_F$ . The back-view generation model is formulated as follows:

$$\hat{\epsilon}_t = \epsilon_{\text{back}}(z_t, I_{\text{A-pose}}, t, I_F, P_F). \quad (8)$$

During training, we observe significant lighting shifts between the front and back camera views in the MVHumanNet dataset. Directly using raw MVHumanNet images introduces color saturation shifts, leading to unrealistic textures in the synthesized back views. To mitigate this issue, we employ the FLUX [Labs 2024] model to enhance the training image quality, particularly in frontal and back A-pose images. As demonstrated in our ablation study in Sec. 4.4, this enhancement significantly improves synthesis quality.

*Stage 3: Free-View & Pose Synthesis.* The final stage generates a human image under an arbitrary pose and viewpoint using the outputs from Stage 1 and Stage 2 along with a pose map. To obtain the foreground segmentation map of  $I_F$  and  $I_B$ , SAM model [Kirillov et al. 2023] is applied to obtain  $P_F$  and  $P_B$ . Thus we have  $I_{\text{free}} = \{I_F, I_B\}$ ,  $P_{\text{free}} = \{P_F, P_B\}$ . The free-view synthesis model is formulated as

Dataset	MVHumanNet [Xiong et al. 2024]				THuman 4.0 [Zheng et al. 2022]				AvatarReX [Zheng et al. 2023]			
Method	FID ↓	LPIPS ↓	PSNR ↑	SSIM ↑	FID ↓	LPIPS ↓	PSNR ↑	SSIM ↑	FID ↓	LPIPS ↓	PSNR ↑	SSIM ↑
AnimateAnyone [Hu 2024]	70.7821	0.4331	13.2582	0.6750	74.1451	0.3642	14.7458	0.7799	69.2732	0.2157	15.5053	0.8264
MagicAnimate [Xu et al. 2024b]	73.4553	0.4798	9.3189	0.7180	96.6649	0.4844	8.3149	0.6974	102.0733	0.5225	7.4551	0.6911
Champ [Zhu et al. 2024]	62.8560	0.3994	13.1042	0.8635	93.3094	0.4457	9.5117	0.7015	78.9367	0.3717	10.4287	0.7676
Ours (SBS)	14.4210	0.1622	17.0370	0.8311	58.5134	0.2262	14.7664	0.7870	53.0746	0.1744	16.1607	0.8378

Table 1. Quantitative evaluation on MVHumanNet [Xiong et al. 2024], THuman 4.0 [Zheng et al. 2022], and AvatarReX dataset [Zheng et al. 2023]. The comparison on THuman 4.0 and AvatarReX is conducted in a zero-shot manner. Cells highlighted in     denotes the best and second-best performances.

follows:

$$\hat{\epsilon}_t = \epsilon_{\text{free}}(z_t, I_{\text{pose}}, t, I_{\text{free}}, P_{\text{free}}). \quad (9)$$

## 4 EXPERIMENTS

### 4.1 Implementation Details

In the implementation of DiscoHuman, both VisualDiT and HumanDiT utilize the pre-trained DiT model from Stable Diffusion 3 Medium [Esser et al. 2024], which consists of 24 DiT blocks. To conserve GPU memory, VisualDiT employs only the first 12 blocks. The corresponding block features  $c^n$  from VisualDiT are duplicated across all blocks to ensure alignment with HumanDiT. The synthesis resolution for the image is set to  $512 \times 768$ . For hyperparameter settings, we use an 8-bit Adam optimizer with a learning rate of  $2 \times 10^{-5}$  and a batch size of 16. All experiments are conducted on two A100 GPUs for 30k training steps.

### 4.2 Dataset

**MVHumanNet.** The MVHumanNet dataset [Xiong et al. 2024] contains multi-view videos of 9,000 subjects with SMPLX and camera annotations. We use 6,000 high-quality subjects to avoid inconsistent camera setups. From each video, we select 8 frames and 4 camera views, yielding 192k training images. For testing, 2 frames and 4 views from 400 subjects result in 3.2k images. Disentangled inputs are extracted from each subject’s A-pose frame using Sapiens [Khrodar et al. 2025], which is excluded from training. **VTON.** This dataset combines VITON-HD [Choi et al. 2021] and DressCode [Morelli et al. 2022], with 60k images and SMPLX estimated via PyMAF-X [Zhang et al. 2023c]. These datasets offer parsing and in-shop clothing annotations but limited views and poses, so we exclude them from evaluation. **THuman 4.0 and AvatarReX.** THuman 4.0 [Zheng et al. 2022] and AvatarReX [Zheng et al. 2023] provide multi-view data for three and four subjects respectively. We select 900 frames in total for zero-shot testing only.

### 4.3 Comparison

In this section, we primarily present the results of the Stage-by-Stage pipeline, as it achieves the best performance. Since Stage 1 (Front-View Synthesis) relies on pre-trained models, we focus our comparison on Stage 2 and Stage 3 to fairly evaluate our contributions. These two stages together can be interpreted as a pose transfer framework, making them directly comparable to SOTA pose transfer methods.

We therefore compare our approach with AnimateAnyone [Hu 2024], MagicAnimate [Xu et al. 2024b], and Champ [Zhu et al. 2024].

Since the official implementation of AnimateAnyone has not been released, we use a third-party reimplementation<sup>1</sup>.

Method	FLUX	FID ↓	LPIPS ↓	PSNR ↑	SSIM ↑
Back-View Model	✓	38.5276	0.1852	15.3949	0.8077
Back-View Model		46.0028	0.1723	15.6032	0.8179
Free-View Model	✓	20.8115	0.1711	16.9394	0.8275
Free-View Model		27.2246	0.1790	15.9477	0.8090

Table 2. Ablation study on FLUX enhancement for back-view model training of the stage-by-stage pipeline. We mark the best results with  .

Method	Training Dataset	FID ↓	LPIPS ↓	PSNR ↑	SSIM ↑
E2E	MVHumanNet + VTON	25.1648	0.4494	10.7573	0.6606
E2E	MVHumanNet	20.7037	0.3747	12.5632	0.7294
SBS	MVHumanNet + VTON	14.4210	0.1622	17.0370	0.8311
SBS	MVHumanNet	20.8115	0.1711	16.9394	0.8275

Table 3. Quantitative results of end-to-end (E2E) vs. stage-by-stage (SBS) training under different dataset combinations. We mark the best and second-best results with    .

**Qualitative Evaluation.** Fig. 4 presents the qualitative results on the MVHumanNet dataset. Our method achieves the best performance across various views and poses. For instance, the first example in the third row of Fig. 4 demonstrates a challenging view and pose transfer. Our model accurately generates the corresponding pose for the given view, whereas other methods fail to synthesize a plausible right leg of the input identity.

In addition to evaluation on MVHumanNet, we assess the zero-shot generalization of our method on the THuman 4.0 [Zheng et al. 2022] and AvatarReX [Zheng et al. 2023] datasets, as shown in Fig. 7. Notably, none of the baselines were trained on these datasets. While Champ delivers comparable texture quality, it fails to accurately capture pose and view variations. Although both our model and Champ adopt SMPLX for pose conditioning, Champ requires stricter inputs such as 2D keypoints and DensePose, making it less robust under challenging poses, views, or unseen domains. AnimateAnyone and MagicAnimate are also less effective at preserving detailed clothing textures. We further validate robustness through zero-shot inference on the People Snapshot dataset [Alldieck et al. 2018], as shown in Fig. 6. Results demonstrate that our stage-by-stage pipeline handles in-the-wild inputs well, achieving accurate pose and view control with strong identity consistency. Notably, although our model is designed for image generation, it consistently produces coherent results across diverse poses and viewpoints, as shown in Fig. 10.

<sup>1</sup>Moore-AnimateAnyone: <https://github.com/MooreThreads/Moore-AnimateAnyone>



Fig. 5. Qualitative comparison for End-to-End (E2E) and Stage-by-Stage (SBS) results on MVHumanNet [Xiong et al. 2024] dataset.

**Quantitative Evaluation.** Tab. 1 presents the quantitative evaluation results of our method. To assess the quality of the synthesized images, we use FID, LPIPS, PSNR, and SSIM as evaluation metrics. Our method achieves the best overall performance across all datasets and metrics.

Notably, the results on THuman 4.0 and AvatarReX are evaluated in a zero-shot setting, further demonstrating the robustness and generalizability of our stage-by-stage (SBS) pipeline. On THuman 4.0 dataset, AnimateAnyone achieves comparable performance in LPIPS, PSNR, and SSIM; however, its FID score is significantly worse than ours, indicating lower perceptual quality. The results show that our method performs consistently well and remains robust across varying numbers of views when generating free-view images. Additionally, Champ achieves the second-best performance on MVHumanNet, suggesting that it is well-suited for scenarios with fewer viewpoints. However, as the number of views increases, AnimateAnyone outperforms Champ and becomes the second-best model. Our method, in contrast, remains robust across different view settings, demonstrating its superior adaptability to view variations.

#### 4.4 Ablation Study

During Stage 2 Back-View Synthesis, we find that directly using a front-view A-pose image to predict its back-view counterpart is highly challenging. This difficulty arises not only from the missing information on the back but also from the inconsistent lighting conditions in the MVHumanNet dataset. As a result, if we explicitly use the synthesized back-view results in Stage 3, we observe a

notable degradation in performance compared to the training setup, which uses a ground-truth A-pose back-view image as input.

To address this, we conduct an ablation study showing that improving the quality of front-back A-pose images significantly benefits both back-view synthesis and free-view generation. As shown in Sec. 4.3, applying FLUX [Labs 2024] to enhance training A-pose images improves FID, with marginal changes in LPIPS, PSNR, and SSIM. Notably, models trained on FLUX-enhanced data (✓ in the FLUX column) yield consistent gains across all metrics when generating free-view images from synthesized back views. As shown in Fig. 8 and Fig. 9, training with FLUX-enhanced data significantly improves the quality of generated hair and clothing textures.

## 5 USER STUDY

We conducted a user study to evaluate the effectiveness of our method on in-the-wild data. We randomly selected 30 cases, each containing four synthesized images generated by the four models under the same input conditions. A total of 50 participants were asked to vote for the image they perceived as the most realistic by considering: view consistency, pose accuracy, identity consistency, and texture fidelity. The results are shown in Tab. 4.

Our Method	AnimateAnyone	MagicAnimate	Champ
61.2%	10.8%	6.6%	21.4%

Table 4. User study results on in-the-wild data. The table shows the percentage of votes received by each method, where a higher percentage indicates stronger user preference.

## 6 DISCUSSION: END-TO-END VS. STAGE-BY-STAGE

The quantitative results of the End-to-End (E2E) pipeline and the Stage-by-Stage (SBS) pipeline are reported in Tab. 3. Comparing the second and fourth rows, both models are trained solely on MVHumanNet, SBS demonstrates significant improvements in LPIPS, PSNR, and SSIM, though it is slightly less effective in FID. This suggests that SBS better preserves pairwise consistency, especially in image quality after pose transfer.

To improve synthesis quality, we incorporate VTON data into training for both E2E and SBS pipelines. However, E2E performance drops after adding VTON (first row), likely due to inconsistent conditioning: MVHumanNet offers rich controls (face, clothing, shoes, pose/view), while VTON is limited to frontal, upper-body photos without faces. To align datasets, missing controls in VTON are set to  $\emptyset$  (e.g., black image) using classifier-free guidance [Ho and Salimans 2022], which introduces misalignment and harms E2E training.

By adopting the stage-by-stage pipeline, we ensure that only Stage 3 (free-view synthesis) is trained on the combined MVHumanNet and VTON datasets. Since VTON lacks front-back A-pose human images, the inputs for front-back view A-pose humans from VTON are set as  $\emptyset$ . Thus, VTON contributes only to pose-to-image training. Compared to E2E framework, which entangles multiple factors, Stage 3 in SBS focuses solely on pose and texture conditioning. This targeted optimization allows the SBS pipeline trained on MVHumanNet and VTON to achieve significant improvements. As

shown in Fig. 5, SBS outperforms E2E, and the strategy trained with VTON dataset produces textures consistent with the ground truth.

## 7 LIMITATIONS AND FUTURE WORK

One limitation of our approach lies in the diffusion model’s tendency to produce artifacts in smaller regions of the image, such as fingers and faces, due to their relatively small size compared to the entire picture. Consequently, the synthesized results from DiscoHuman occasionally exhibit imperfections in these areas. However, this limitation can be mitigated through post-processing methods that do not require additional fine-tuning. For example, utilizing the ADetailer plugin<sup>2</sup> effectively addresses these artifacts. This plugin regenerates the face and hand regions with a larger cropped resolution and seamlessly pastes the improved regions back into the original image, significantly enhancing the overall quality. Future work could explore integrating such post-processing techniques directly into the generation pipeline for a more streamlined and robust output.

## 8 CONCLUSION

We introduce a new and challenging task in human image synthesis that controls viewpoint, pose, clothing, and identity within a unified framework. While an end-to-end model offers a straightforward approach, our analysis reveals its limitations in generalizability, particularly when trained on datasets with inconsistent conditioning factors. To address this, we propose a stage-by-stage framework, which significantly enhances pose and viewpoint control while improving robustness to in-the-wild scenarios. Our experiments demonstrate that structured factor disentanglement leads to improved synthesis quality, particularly in zero-shot settings. By leveraging dataset specialization in different stages, our method enables more effective utilization of available data, outperforming existing approaches in view and pose control. However, our approach is still limited by the diffusion model’s tendency to produce artifacts in small regions (e.g., fingers and faces) due to their relative size. We will resolve this in future work. We hope our findings on end-to-end vs. stage-by-stage synthesis will inspire further research in controllable human generation.

## REFERENCES

Thiemo Alldieck, Marcus Magnor, Weipeng Xu, Christian Theobalt, and Gerard Pons-Moll. 2018. Video Based Reconstruction of 3D People Models. In *CVPR*.  
 Sizhe An, Hongyi Xu, Yichun Shi, Guoxian Song, Umit Y. Ogras, and Linjie Luo. 2023. PanoHead: Geometry-Aware 3D Full-Head Synthesis in 360deg. In *Computer Vision and Pattern Recognition (CVPR)*.  
 Qingyan Bai and Yujun Shen. 2024. Real-time 3D-aware Portrait Editing from a Single Image. *ArXiv* (2024).  
 Ankan Kumar Bhunia, Salman Khan, Hisham Cholakkal, Rao Muhammad Anwer, Jorma Laaksonen, Mubarak Shah, and Fahad Shahbaz Khan. [n. d.]. Person image synthesis via denoising diffusion model. In *CVPR*.  
 Eric R. Chan, Connor Z. Lin, Matthew A. Chan, Koki Nagano, Boxiao Pan, Shalini De Mello, Orazio Gallo, Leonidas J. Guibas, Jonathan Tremblay, Sameh Khamis, Tero Karras, and Gordon Wetzstein. 2022. Efficient Geometry-Aware 3D Generative Adversarial Networks. In *CVPR*.  
 Seunghwan Choi, Sunghyun Park, Minsoo Lee, and Jaegul Choo. 2021. VITON-HD: High-Resolution Virtual Try-On via Misalignment-Aware Normalization. In *Proceedings of the IEEE/CVF Conference on Computer Vision and Pattern Recognition*.  
 Yunje Choi, Minje Choi, Munyoung Kim, Jung-Woo Ha, Sunghun Kim, and Jaegul Choo. 2018. StarGAN: Unified Generative Adversarial Networks for Multi-Domain Image-to-Image Translation. In *CVPR*.

Yisul Choi, Sangkyung Kwak, Kyungmin Lee, Hyungwon Choi, and Jinwoo Shin. 2025. Improving Diffusion Models for Authentic Virtual Try-on in the Wild. In *Computer Vision – ECCV 2024*, Aleš Leonardis, Elisa Ricci, Stefan Roth, Olga Russakovsky, Torsten Sattler, and Gül Varol (Eds.). Springer Nature Switzerland, Cham, 206–235.  
 Zijian Dong, Xu Chen, Jinlong Yang, Michael J Black, Otmar Hilliges, and Andreas Geiger. 2023. Ag3d: Learning to generate 3d avatars from 2d image collections. In *Proceedings of the IEEE/CVF international conference on computer vision*.  
 Patrick Esser, Sumith Kulal, Andreas Blattmann, Rahim Entezari, Jonas Müller, Harry Saini, Yam Levi, Dominik Lorenz, Axel Sauer, Frederic Boesel, et al. 2024. Scaling rectified flow transformers for high-resolution image synthesis. In *Forty-first International Conference on Machine Learning*.  
 Anna Frühstück, Krishna Kumar Singh, Eli Shechtman, Niloy J. Mitra, Peter Wonka, and Jingwan Lu. 2022. InsetGAN for Full-Body Image Generation. In *Proceedings of the IEEE/CVF Conference on Computer Vision and Pattern Recognition (CVPR)*. 7723–7732.  
 Jianglin Fu, Shikai Li, Yuming Jiang, Kwan-Yee Lin, Chen Qian, Chen Change Loy, Wayne Wu, and Ziwei Liu. 2022. StyleGAN-Human: A Data-Centric Odyssey of Human Generation. In *Computer Vision – ECCV 2022*.  
 Ian Goodfellow, Jean Pouget-Abadie, Mehdi Mirza, Bing Xu, David Warde-Farley, Sherjil Ozair, Aaron Courville, and Yoshua Bengio. 2014. Generative adversarial nets. *Advances in neural information processing systems* 27 (2014).  
 Jonathan Ho and Tim Salimans. 2022. Classifier-free diffusion guidance. *arXiv preprint arXiv:2207.12598* (2022).  
 Fangzhou Hong, Zhaoxi Chen, Yushi LAN, Liang Pan, and Ziwei Liu. 2023. EVA3D: Compositional 3D Human Generation from 2D Image Collections. In *The Eleventh International Conference on Learning Representations*.  
 Li Hu. 2024. Animate anyone: Consistent and controllable image-to-video synthesis for character animation. In *Proceedings of the IEEE/CVF Conference on Computer Vision and Pattern Recognition*. 8153–8163.  
 Tero Karras, Timo Aila, Samuli Laine, and Jaakko Lehtinen. 2018. Progressive Growing of GANs for Improved Quality, Stability, and Variation. In *International Conference on Learning Representations*. <https://openreview.net/forum?id=Hk99zCeAb>  
 Tero Karras, Samuli Laine, and Timo Aila. 2019. A Style-Based Generator Architecture for Generative Adversarial Networks. In *Proceedings of the IEEE/CVF Conference on Computer Vision and Pattern Recognition (CVPR)*.  
 Tero Karras, Samuli Laine, Miika Aittala, Janne Hellsten, Jaakko Lehtinen, and Timo Aila. 2020. Analyzing and Improving the Image Quality of StyleGAN. In *Proceedings of the IEEE/CVF Conference on Computer Vision and Pattern Recognition (CVPR)*.  
 Rawal Khrodgar, Timur Bagautdinov, Julieta Martinez, Su Zhaoen, Austin James, Peter Selednik, Stuart Anderson, and Shunsuke Saito. 2025. Sapiens: Foundation for Human Vision Models. In *European Conference on Computer Vision*. Springer.  
 Alexander Kirillov, Eric Mintun, Nikhila Ravi, Hanzi Mao, Chloe Rolland, Laura Gustafson, Tete Xiao, Spencer Whitehead, Alexander C. Berg, Wan-Yen Lo, Piotr Dollar, and Ross Girshick. 2023. Segment Anything. In *Proceedings of the IEEE/CVF International Conference on Computer Vision (ICCV)*. 4015–4026.  
 Black Forest Labs. 2024. FLUX. <https://github.com/black-forest-labs/flux>.  
 Sangyun Lee, Gyojung Gu, Sunghyun Park, Seunghwan Choi, and Jaegul Choo. 2022. High-resolution virtual try-on with misalignment and occlusion-handled conditions. In *European Conference on Computer Vision*. Springer, 204–219.  
 Chenghong Li, Hongjie Liao, Yihao Zhi, Xihe Yang, Zhengwentai Sun, Jiahao Chang, Shuguang Cui, and Xiaoguang Han. 2025. MVHumanNet++: A Large-scale Dataset of Multi-view Daily Dressing Human Captures with Richer Annotations for 3D Human Digitization. *arXiv preprint arXiv:2505.01838* (2025).  
 Heyuan Li, Ce Chen, Tianhao Shi, Yuda Qiu, Sizhe An, Guanying Chen, and Xiaoguang Han. 2024. SphereHead: Stable 3D Full-head Synthesis with Spherical Tri-plane Representation. *arXiv:2404.05680 [cs.CV]*  
 Connor Z. Lin, David B. Lindell, Eric Chan, and Gordon Wetzstein. 2022. 3D GAN Inversion for Controllable Portrait Image Animation. *ArXiv abs/2203.13441* (2022). <https://api.semanticscholar.org/CorpusID:247748597>  
 Xingchao Liu, Chengyue Gong, and Qiang Liu. 2022. Flow straight and fast: Learning to generate and transfer data with rectified flow. *arXiv preprint arXiv:2209.03003* (2022).  
 Ziwei Liu, Ping Luo, Xiaogang Wang, and Xiaoou Tang. 2015. Deep Learning Face Attributes in the Wild. In *IEEE International Conference on Computer Vision*.  
 Yongyi Lu, Yu-Wing Tai, and Chi-Keung Tang. 2018. Attribute-Guided Face Generation Using Conditional CycleGAN. In *ECCV*.  
 Yanzuo Lu, Manlin Zhang, Andy J Ma, Xiaohua Xie, and Jianhuang Lai. 2024. Coarse-to-fine latent diffusion for pose-guided person image synthesis. In *Proceedings of the IEEE/CVF Conference on Computer Vision and Pattern Recognition*. 6420–6429.  
 Davide Morelli, Matteo Fincato, Marcella Cornia, Federico Landi, Fabio Cesari, and Rita Cucchiara. 2022. Dress Code: High-Resolution Multi-Category Virtual Try-On. In *CVPR Workshops*.  
 Georgios Pavlakos, Vasileios Choutas, Nima Ghorbani, Timo Bolkart, Ahmed A. A. Osman, Dimitrios Tzionas, and Michael J. Black. 2019. Expressive Body Capture: 3D Hands, Face, and Body From a Single Image. In *Proceedings of the IEEE/CVF Conference on Computer Vision and Pattern Recognition (CVPR)*. 10975–10985.

<sup>2</sup>ADetailer plugin: <https://github.com/Bing-su/adetailer>

- William Peebles and Saining Xie. 2023. Scalable Diffusion Models with Transformers. In *Proceedings of the IEEE/CVF International Conference on Computer Vision (ICCV)*.
- Kripasindhu Sarkar, Lingjie Liu, Vladislav Golyanik, and Christian Theobalt. 2021. HumanGAN: A Generative Model of Human Images. In *2021 International Conference on 3D Vision (3DV)*. 258–267. <https://doi.org/10.1109/3DV53792.2021.00036>
- Ruizhi Shao, Youxin Pang, Zerong Zheng, Jingxiang Sun, and Yebin Liu. 2024. Human4dit: 360-degree human video generation with 4d diffusion transformer. *arXiv preprint arXiv:2405.17405* (2024).
- Fei Shen, Hu Ye, Jun Zhang, Cong Wang, Xiao Han, and Wei Yang. 2023. Advancing pose-guided image synthesis with progressive conditional diffusion models. *arXiv preprint arXiv:2310.06313* (2023).
- Jiaxin Xie, Hao Ouyang, Jintan Piao, Chenyang Lei, and Qifeng Chen. 2023. High-fidelity 3d gan inversion by pseudo-multi-view optimization. In *Proceedings of the IEEE/CVF Conference on Computer Vision and Pattern Recognition*. 321–331.
- Zhangyang Xiong, Di Kang, Derong Jin, Weikai Chen, Linchao Bao, Shuguang Cui, and Xiaoguang Han. 2023. Get3dhuman: Lifting stylegan-human into a 3d generative model using pixel-aligned reconstruction priors. In *ICCV*.
- Zhangyang Xiong, Chenghong Li, Kenkun Liu, Hongjie Liao, Jianqiao Hu, Junyi Zhu, Shuliang Ning, Lingteng Qiu, Chongjie Wang, Shijie Wang, Shuguang Cui, and Xiaoguang Han. 2024. MVHumanNet: A Large-scale Dataset of Multi-view Daily Dressing Human Captures. In *Proceedings of the IEEE/CVF Conference on Computer Vision and Pattern Recognition (CVPR)*. 19801–19811.
- Yuhao Xu, Tao Gu, Weifeng Chen, and Chengcai Chen. 2024a. Ootdiffusion: Outfitting fusion based latent diffusion for controllable virtual try-on. *arXiv preprint arXiv:2403.01779* (2024).
- Zhongcong Xu, Jianfeng Zhang, Jun Hao Liew, Hanshu Yan, Jia-Wei Liu, Chenxu Zhang, Jiashi Feng, and Mike Zheng Shou. 2024b. Magicanimate: Temporally consistent human image animation using diffusion model. In *Proceedings of the IEEE/CVF Conference on Computer Vision and Pattern Recognition*. 1481–1490.
- Shuai Yang, Zhangyang Wang, Jiaying Liu, and Zongming Guo. 2020. Deep plastic surgery: Robust and controllable image editing with human-drawn sketches. In *ECCV*. Springer.
- Hu Ye, Jun Zhang, Sibao Liu, Xiao Han, and Wei Yang. 2023. Ip-adapter: Text compatible image prompt adapter for text-to-image diffusion models. *arXiv preprint* (2023).
- Chi Zhang, Yiwen Chen, Yijun Fu, Zhenglin Zhou, Gang Yu, Billz Wang, Bin Fu, Tao Chen, Guosheng Lin, and Chunhua Shen. 2023a. Styleavatar3d: Leveraging image-text diffusion models for high-fidelity 3d avatar generation. *arXiv preprint arXiv:2305.19012* (2023).
- Hongwen Zhang, Yating Tian, Yuxiang Zhang, Mengcheng Li, Liang An, Zhenan Sun, and Yebin Liu. 2023c. Pymaf-x: Towards well-aligned full-body model regression from monocular images. *IEEE TPAMI* (2023).
- Lvmin Zhang, Anyi Rao, and Maneesh Agrawala. 2023b. Adding Conditional Control to Text-to-Image Diffusion Models. In *Proceedings of the IEEE/CVF International Conference on Computer Vision (ICCV)*. 3836–3847.
- Xuanmeng Zhang, Jianfeng Zhang, Rohan Chacko, Hongyi Xu, Guoxian Song, Yi Yang, and Jiashi Feng. 2023d. Getavatar: Generative textured meshes for animatable human avatars. In *IEEE/CVF International Conference on Computer Vision*.
- Zerong Zheng, Han Huang, Tao Yu, Hongwen Zhang, Yandong Guo, and Yebin Liu. 2022. Structured local radiance fields for human avatar modeling. In *Proceedings of the IEEE/CVF Conference on Computer Vision and Pattern Recognition*. 15893–15903.
- Zerong Zheng, Xiaochen Zhao, Hongwen Zhang, Boning Liu, and Yebin Liu. 2023. Avatarrex: Real-time expressive full-body avatars. *ACM Transactions on Graphics (TOG)* 42, 4 (2023), 1–19.
- Shenhao Zhu, Junming Leo Chen, Zuozhuo Dai, Zilong Dong, Yinghui Xu, Xun Cao, Yao Yao, Hao Zhu, and Siyu Zhu. 2024. Champ: Controllable and consistent human image animation with 3d parametric guidance. In *ECCV*. Springer.



Fig. 6. Given a reference person image from the People Snapshot dataset [Alldieck et al. 2018] (leftmost in each sample) and a target pose (visualized as a colored SMPLX body map), our method (Stage-by-Stage pipeline) synthesizes the same person performing the new action from a specified novel view. Note that our model is evaluated in a zero-shot setting on this dataset, demonstrating strong generalization in pose transfer and view synthesis.



Fig. 7. Qualitative comparison of different methods on sampled results from THuman4.0 [Zheng et al. 2022] (bottom) and AvatarRex [Zheng et al. 2023] (top) datasets. Note that AA stands for AnimateAnyone and MA stands for MagicAnimate.

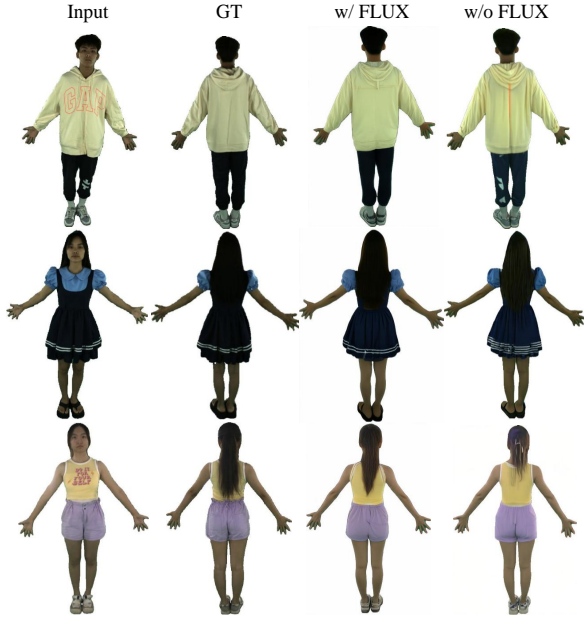


Fig. 8. Ablation results of back-view synthesis models trained with and without FLUX-enhanced data.

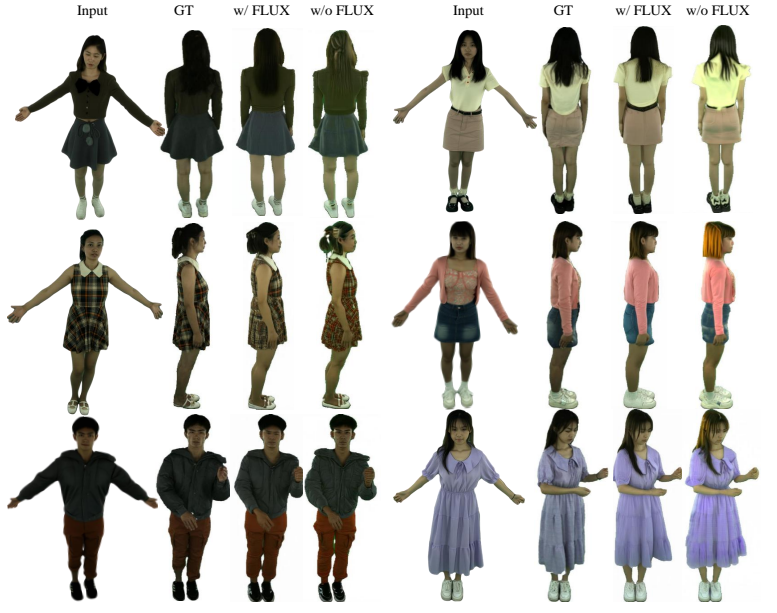


Fig. 9. Free-view synthesis results based on back-view models trained with and without FLUX-enhanced data.

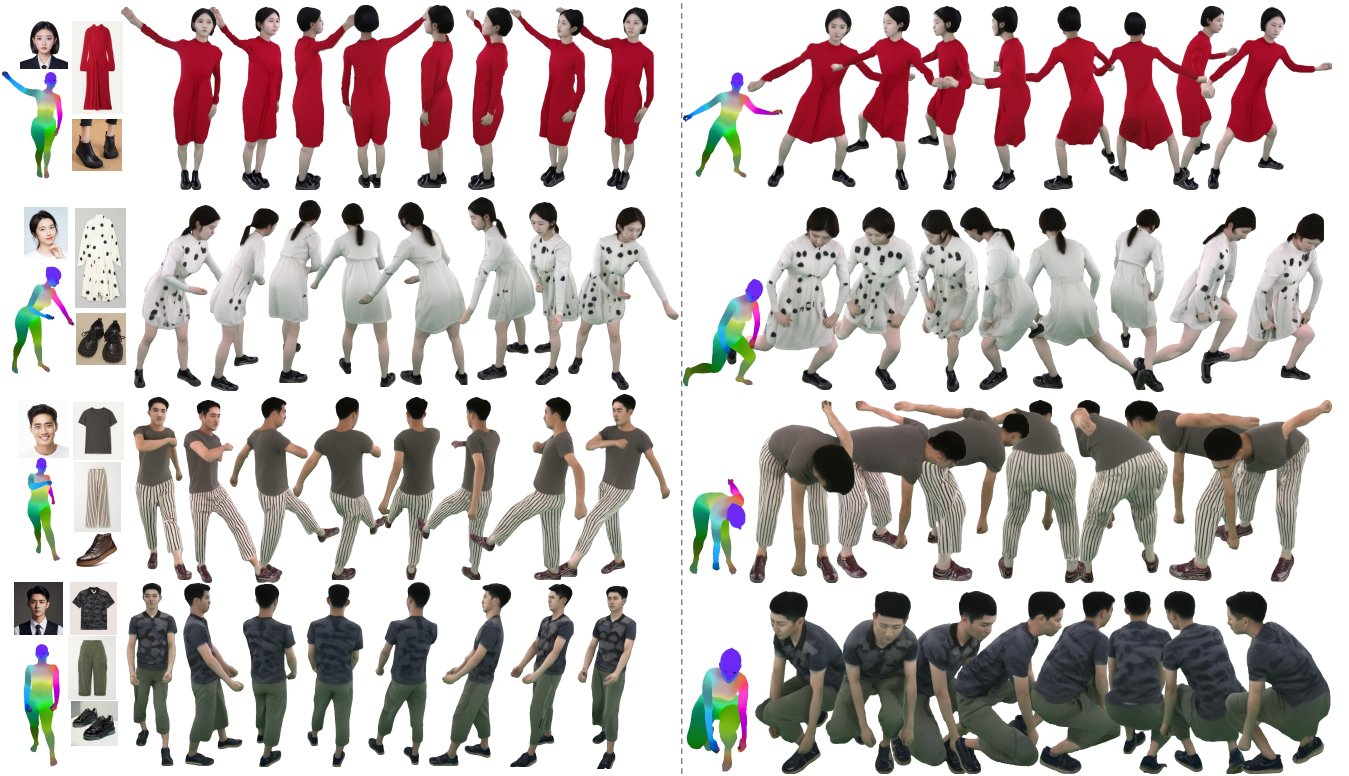


Fig. 10. View interpolation results achieved by the Stage-by-Stage (SBS) pipeline. Each row shows synthesized images of the same identity and clothing under two poses and multiple viewpoints. Despite being an image generation model, DiscoHuman produces smooth and consistent transitions across views, demonstrating strong continuity and factor disentanglement.